Cardiovascular Revascularization Medicine 20 (2019) 485–491

Contents lists available at ScienceDirect

Cardiovascular Revascularization Medicine

Major coronary evaginations following implantation of bioresorbable vascular scaffolds – Clinical and OCT characteristics

Florian Blachutzik [a,b,*], Stephan Achenbach [b], Mohamed Marwan [b], Jens Röther [b], Monique Tröbs [b], Reinhard Schneider [b], Holger Nef [a], Melissa Weissner [c,d], Christian Schlundt [b]

[a] Justus-Liebig University Giessen, Medizinische Klinik 1, Department of Cardiology, Giessen, Germany
[b] Friedrich-Alexander Universität (FAU) Erlangen-Nürnberg, University Hospital Erlangen, Department of Cardiology, Erlangen, Germany
[c] Zentrum für Kardiologie, University Hospital Mainz, Mainz, Germany
[d] German Center for Cardiac and Vascular Research (DZHK), Standort Rhein-Main, Mainz, Germany

ARTICLE INFO

Article history:
Received 27 April 2018
Received in revised form 27 July 2018
Accepted 1 August 2018

Keywords:
Percutaneous coronary intervention
Optical coherence tomography
Bioresorbable vascular scaffolds

ABSTRACT

Background: Coronary evaginations can occur after implantation of bioresorbable vascular scaffolds (BRS) and may be associated with scaffold thrombosis. Aim of this study was to clarify the clinical manifestation, extent and time course of coronary artery remodeling in vessel segments that develop angiographically detectable evaginations following BRS implantation through optical coherence tomography (OCT) analysis.
Methods: In 8 patients, 10 BRS (Absorb, Abbott Vascular, Santa Clara, CA, USA) which displayed coronary evaginations in clinically driven late invasive coronary angiograms were identified and findings were compared to 10 BRS in 8 patients without coronary evaginations. Vessel and device geometry was analyzed in serial OCT cross-sections at a spacing of 200 μm. Measured BRS dimensions were normalized to the reference vessel size at implantation.
Results: In OCT, major evaginations on average affected 24 ± 19% of the scaffold length. Scaffolds with major evaginations had a significantly larger lumen area than scaffolds without evaginations (mean normalized lumen area 1.19 ± 0.58 vs. 0.77 ± 0.38; $p < 0.001$), and also displayed a significantly larger scaffold area (mean normalized scaffold area: 1.36 ± 0.6 vs. 1.13 ± 0.43; $p < 0.001$), and scaffold diameter (mean normalized scaffold diameter: 1.17 ± 0.33 vs.1.04 ± 0.19; $p < 0.001$). Lumen area ($r = 0.47$; $p < 0.001$), scaffold area ($r = 0.52$; $p < 0.001$), and scaffold diameter ($r = 0.74$; $p < 0.001$) in the evagination group were positively correlated to the time since scaffold implantation.
Conclusion: Coronary evaginations following BRS implantation are associated with an increased scaffold area, indicating that the scaffold follows the outward remodeling of the artery. The process affects the entire scaffold length and seems to be continuously progressing following implantation.

1. Introduction

Bioresorbable vascular scaffolds (BRS) have been introduced into clinical practice in 2012. In contrast to conventional metallic stents, BRS are resorbed over the course of time and thus thought to restore vessel pulsatility, cyclical strain, physiological shear stress, and mechanotransduction [1,2]. Recent findings suggest that coronary evaginations may occur after implantation of BRS [3]. Coronary evaginations had initially been described as a specific optical coherence tomography (OCT) finding after implantation of first generation drug-eluting stents (DES). They have been assumed to be associated to vessel injury at implantation, display positive remodeling of the vessel wall during further course and correlate with uncovered stent struts, strut fractures and malapposition [4–7]. Coronary evaginations disturb laminar flow and have been reported as possible risk factor for late stent thrombosis [8,9]. Evaginations are nearly absent in newer generation DES, which may contribute to their lower rate of late stent thrombosis in comparison to first generation DES [4]. Recent publications report cases of coronary aneurysms following BRS implantation [10–12]. We hypothesize that these cases may be the end stage of evaginations in which the scaffold, due to loss of mechanical integrity, has expanded to follow extreme outward remodeling of the vessel wall. In this study, we therefore analyze clinical and morphological features of major evaginations associated with BRS and, to elucidate the dynamics of vessel remodeling and scaffold dimensions in patients who develop evaginations, we report the relationship of coronary evaginations, vessel dimensions, and scaffold geometry, as well as their development over time.

* Corresponding author at: University Hospital Giessen, Department of Cardiology, Klinikstrasse 33, 35392 Giessen, Germany.
E-mail address: florian.blachutzik@innere.med.uni-giessen.de (F. Blachutzik).

https://doi.org/10.1016/j.carrev.2018.08.001
1553-8389/

2. Materials and methods

2.1. Study design and population

We retrospectively analyzed all patients who underwent repeat coronary angiography after prior PCI with implantation of at least one BRS in our department between December 2014 and July 2016. All angiograms were clinically driven. In 8 out of 94 patients, evaginations were identified angiographically because of peri-stent contrast staining in the segment of previously implanted BRS and were confirmed by OCT. For the purpose of further analysis, evaginations were defined as "present" in OCT when the vessel contour extended beyond the outer border of well-apposed struts (see Fig. 1) [3]. If evaginations were identified angiographically, performance of OCT was obligatory per institutional protocol. In all other cases, performance of OCT was at the discretion of the operator. In 20 out of the 86 patients without coronary evaginations at the time of repeat angiography OCT was performed. 8 of these 20 patients, matched for the time since BRS implantation, served as control group. Baseline characteristics of the patients, including medical history as well as clinical, angiographic, and procedural data, were collected from the department's database.

2.2. Percutaneous coronary intervention

Baseline PCI with implantation of a BRS had been performed via transradial or transfemoral approach using 6 French guiding catheters and standard coronary guidewires (Runthrough™, Terumo Europe NV, Leuven, Belgium). All patients had received intravenous heparin and intracoronary nitrates. Pre-dilatation with a non-compliant balloon (NC balloon) had been performed in all lesions, with balloon size selected based on visual angiographic estimation to achieve a 1:1 ratio of vessel and balloon diameter. Lesions had been treated with everolimus-eluting BRS (Absorb BVS™, Abbott Vascular, Santa Clara, CA, USA). Deployment of Absorb BVS™ had been performed with an initial pressure of 2 bar and increasing pressure in increments of 2 bar every 10 s until fully deployed (minimum 8 bar). Further medication, techniques, and equipment for PCI were used in accordance with current clinical guidelines and were left to the responsible physician's discretion. NC balloon (NC Trek™, Abbott Vascular, Santa Clara, CA, USA) post-dilatation at a pressure of 16 bar was mandatory per institutional protocol and had been performed in all lesions.

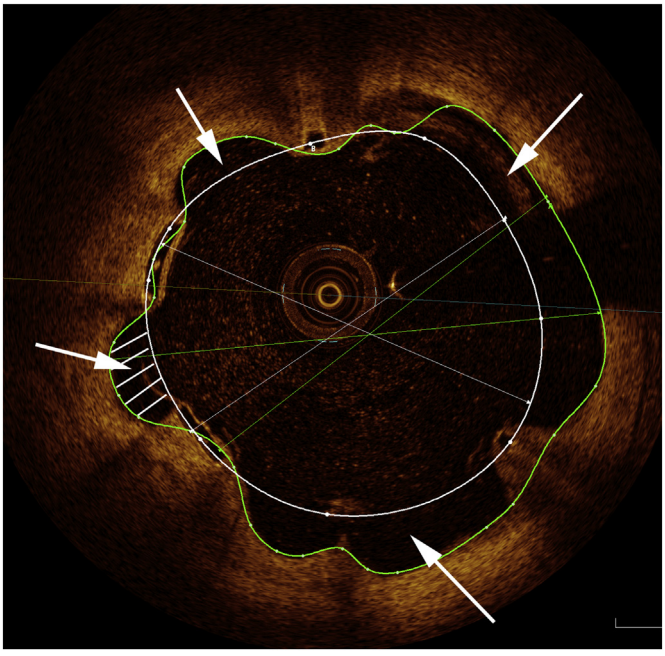

Fig. 1. Analysis of OCT cross section. Absorb BVS™ showing peri-scaffold evaginations (white arrows). The lumen area is contoured in green, the scaffold area is contoured in white. The area of one evagination is hatched in white.

2.3. Optical coherence tomography image acquisition

At follow-up, OCT was performed as part of the diagnostic angiogram and before any PCI. A 2.7 French Dragonfly™ intravascular imaging catheter (St. Jude Medical, Saint Paul, MN, USA) was used with a mechanical pullback speed of 18 mm/s over a distance of 54 mm. During pullback, 25 ml contrast agent (Ultravist™ 370, Bayer AG, Leverkusen, Germany) were injected at 4 ml/s with a maximum pressure of 400 psi using machine injection (Liebel-Flarsheim 903300 G, Liebel-Flarsheim Co, Cincinnati, OH, USA).

2.4. Optical coherence tomography image analysis

All OCT data sets were digitally recorded, stored, and analyzed. OCT image analysis was performed offline using the ILUMIEN™ OPTIS™ system (St. Jude Medical, Saint Paul, MN, USA) with manual calibration before each measurement. OCT cross sections were analyzed over the complete length of implanted BRS with a spacing of 200 μm. Malapposition was defined as any visible malapposition between the abluminal strut edge and the vessel wall. Strut fractures were defined as struts lying isolated in the lumen or the presence of one strut on top of another. Evaginations were defined as "present" when the vessel contour extended beyond the outer border of well-apposed struts [3]. Maximum evagination depth was measured between the direct connection line of the outer edge of two adjacent struts and the vessel wall. The area between the vessel wall and the above-mentioned connection line was measured by manual tracing and represented the evagination area (see Fig. 1). Evaginations can be differentiated from neointimal coverage of malapposed struts with abluminal connecting bridge since evaginations are usually visible all around the vessel circumference. Additionally, scaffold struts next to evaginations are usually well embedded into the vessel wall, whereas malapposed struts usually only have a thin layer of neointimal coverage. Eccentricity index was defined as the ratio between the minimum and maximum scaffold diameter. Lumen area was traced by following the vessel's intima. Scaffold area was traced by connecting the abluminal edges of the scaffold struts. OCT analysis was performed in accordance with previous publications [3,13]. All diameters and lumen or scaffold areas were normalized to the reference vessel size at implantation as determined by quantitative coronary angiography (QCA). Reference vessel size at baseline was obtained by QCA. Mean reference vessel size was calculated over the complete length of the coronary segment to be treated. Normalization was performed by dividing lumen and scaffold dimensions at follow-up through reference vessel size at baseline.

2.5. Statistical analysis

Continuous variables are summarized as mean ± standard deviation; categorical variables are provided as *n* (%). The Kolmogorov-Smirnov test was performed to test for non-parametric distribution. To test for statistical differences between two groups for comparison of continuous variables, either a *t*-test for unpaired samples (parametric distribution) or a Mann-Whitney-*U* test (non-parametric distribution) was used. For categorical variables, a Chi-squared or a Fisher's exact test was carried out. The Pearson correlation coefficient was calculated to analyze linear relationships. Statistical analyses were performed using SPSS version 21.0 (IBM SPSS Statistics, IBM Corporation, Armonk, New York, USA). A two-sided $p < 0.05$ was considered significant.

3. Results

3.1. Patients and clinical parameters

16 patients, 8 with and 8 without coronary evaginations after BRS implantation were included in this study. In one patient out of the evagination group, peri-scaffold evaginations were present in two BRS implanted in different vessels, in another patient out of the evagination group, peri-scaffold evaginations were present in two BRS implanted in the same vessel. The mean interval since BRS implantation was 17 ± 9 months for the evagination group and 18 ± 11 months for the control group. In all patients, follow-up had been clinically driven. Antiplatelet therapy with acetylsalicylic acid plus clopidogrel, ticagrelor or prasugrel had been prescribed for 12 months after the initial BRS implantation. There were no significant differences between the groups regarding baseline characteristics. For detailed patient characteristics see Table 1.

At follow-up, one patient out of the control group presented with non-ST-segment elevation myocardial infarction (NSTEMI), the other 7 patients because of stable angina. 5 of these 7 patients had a proven myocardial ischemia (stress echocardiography, SPECT myocardial perfusion or adenosine stress cardiac magnetic resonance). In the evagination group, one patient presented with NSTEMI, 7 patients presented with stable angina. 4 of these 7 patients had ischemia in noninvasive testing. In 10 of 16 patients, PCI was performed. In 5 of 8 patients in the evagination group and in 3 of 8 patients in the control group, this concerned the vessel in which a BRS had been implanted at baseline ($p = 0.62$). The index lesion was revascularized in 3 of 8 patients in the evagination group and in 3 of 8 patients in the control group ($p > 0.99$), in 2 cases DES and in 1 case Bare-metal stents (BMS) were implanted within the scaffold. In the evagination group, 2 of 3 stent implantations were performed specifically as an attempt to treat evaginations and 1 of 3 due to in-scaffold restenosis. In the control group, all 3 stent implantations were performed due to in-scaffold restenosis. For detailed outcome results see Table 2.

3.2. Baseline percutaneous coronary intervention

NC balloon pre-dilatation and post-dilatation had been performed in all cases during baseline implantation of a bioresorbable scaffold. Mean NC balloon diameter for pre-dilatation was 2.9 ± 0.5 mm. Mean scaffold diameter was 3.2 ± 0.4 mm in the evagination group and 3.1 ± 0.4 mm in the control group ($p = 0.92$). Mean NC balloon diameter for post-dilatation was 3.1 ± 1.2 mm. Bailout stenting was not necessary in any of the cases. In one patient of the control group, two BRS were implanted overlapping each over using the “marker to marker” method. For detailed procedural characteristics see Table 3.

3.3. Optical coherence tomography data – evagination vs. control group

As an effect of outward vessel expansion, mean lumen area normalized to baseline was significantly larger in BRS with evaginations as compared to BRS in the control group (1.19 ± 0.58 vs. 0.77 ± 0.38; $p < 0.001$). Scaffolds also displayed expansion: mean scaffold area normalized to the baseline value at implantation (1.36 ± 0.60 vs. 1.13 ± 0.43; $p < 0.001$), and scaffold diameter normalized to baseline (1.17 ± 0.33 vs. 1.04 ± 0.19; $p < 0.001$) were significantly larger in the evagination group as compared to the control group. Additionally, strut

Table 1
Patient characteristics.

Variable	All patients ($n = 16$)	Evagination group ($n = 8$)	Control group ($n = 8$)	p-Value
Age (years)	63 ± 7	63 ± 6	63 ± 7	0.93
Male/female	11/5	7/1	4/4	0.28
Body-Mass-Index (kg/m^2)	29.5 ± 7.2	29.4 ± 4.8	29.5 ± 6.6	0.78
Clinical presentation				
Stable angina	11 (69%)	5 (62.5%)	6 (75%)	0.72
Unstable angina	2 (12%)	1 (12.5%)	1 (12.5%)	
Non-ST-segment elevation myocardial infarction	3 (19%)	2 (25%)	1 (12.5%)	
Left ventricular ejection fraction (%)	47 ± 8	46 ± 6	48 ± 9	0.34
Left ventricular ejection fraction <30%	0 (0%)	0 (0%)	0 (0%)	>0.99
Hypertension	10 (63%)	4 (50%)	6 (75%)	0.22
Diabetes	4 (25%)	2 (25%)	2 (25%)	>0.99
Family history	8 (50%)	3 (37.5%)	5 (62.5%)	0.18
Hyperlipidaemia	15 (94%)	7 (87.5%)	8 (100%)	0.84
Active smoking	5 (31%)	3 (37.5%)	2 (25%)	0.74
Previous myocardial infarction	2 (12.5%)	1 (12.5%)	1 (12.5%)	>0.99
Previous percutaneous coronary intervention	5 (31%)	2 (25%)	3 (37.5%)	0.74
Previous coronary bypass surgery	2 (12.5%)	1 (12.5%)	1 (12.5%)	>0.99
Atrial fibrillation	2 (12.5%)	1 (12.5%)	1 (12.5%)	>0.99
Time since scaffold implantation (months)				
Mean	18	17	18	0.84
Minimum	4	4	9	
Maximum	33	33	33	
Target lesion				
Left anterior descending artery	5 (30%)	2 (22%)	3 (37.5%)	0.43
Circumflex artery	6 (35%)	3 (33%)	3 (37.5%)	
Right coronary artery	6 (35%)	4 (45%)	2 (25%)	
Lesion type (ACC/AHA-classification)				
A	0 (0%)	0 (0%)	0 (0%)	0.45
B1	2 (11%)	2 (20%)	0 (0%)	
B2	12 (67%)	7 (70%)	5 (62.5%)	
C	4 (22%)	1 (10%)	3 (37.5%)	
Antiplatelet therapy				
Acetylsalicylic acid	16 (100%)	8 (100%)	8 (100%)	>0.99
Clopidogrel	7 (37.5%)	3 (37.5%)	4 (50%)	0.80
Ticagrelor	6 (37.5%)	3 (37.5%)	3 (37.5%)	>0.99
Prasugrel	3 (25%)	2 (25%)	1 (12.5%)	0.74

Values are mean ± standard deviation or n (%).

Table 2
Outcome ($n = 16$).

Variable	Evagination group ($n = 8$)	Control group ($n = 8$)	p-Value
Clinical presentation			
Stable angina	7/8 (87.5%)	7/8 (87.5%)	>0.99
Non-ST-segment elevation myocardial infarction	1/8 (12.5%)	1/8 (12.5%)	
Target vessel myocardial infarction	1/8 (12.5%)	1/8 (12.5%)	>0.99
Any percutaneous revascularization	7/8 (87.5%)	3/8 (37.5%)	0.12
Target vessel revascularization	5/8 (62.5%)	3/8 (37.5%)	0.62
Target lesion revascularization	3/8 (37.5%)	3/8 (37.5%)	>0.99
Stent implantation over scaffold	3/8 (37.5%)	3/8 (37.5%)	>0.99
Reason for target lesion revascularization			
Evaginations	2/3 (67%)	0/3 (0%)	0.4
In-scaffold re-stenosis	1/3 (33%)	3/3 (100%)	0.14
Type of stent implanted over scaffold			
Bare-metal stent	1/3 (33%)	0/3 (0%)	0.82
Drug-eluting stent	2/3 (67%)	3/3 (100%)	0.79

Values are n (%).

fractures (0.08 ± 0.11 vs. 0.02 ± 0.18; $p = 0.03$) and malapposed struts (0.13 ± 0.24 vs. 0.03 ± 0.07; $p = 0.006$) were detected significantly more frequently in the evagination group. For detailed results see Table 4.

3.4. Optical coherence tomography data – BRS with evaginations

In the evagination group, peri-scaffold evaginations were visible over $24 \pm 19\%$ of the complete BRS length (minimum: 12%, maximum: 59%). Cross-sections with evaginations had a mean evagination area of 0.96 ± 1 mm^2 and a mean evagination depth of 0.48 ± 0.2 mm. Lumen area normalized to baseline was significantly larger in segments affected by evaginations as compared to those without (1.38 ± 0.49 vs. 1.13 ± 0.59; $p < 0.001$). Scaffold expansion was observed along the entire length of BRS affected by evaginations: scaffold diameter (1.18 ± 0.33 vs. 1.16 ± 0.20, $p = 0.33$) and consecutively, scaffold area normalized to baseline (1.37 ± 0.45 vs. 1.36 ± 0.64; $p = 0.41$), were only very slightly larger in areas with coronary evagination as compared to areas without. The frequency of strut fractures (0.23 ± 0.31 per cross-section vs. 0.07 ± 0.14 per cross-section; $p = 0.02$) as well as of malapposed struts (0.41 ± 0.36 vs. 0.13 ± 0.07 per cross-section; $p = 0.003$) was significantly higher in evagination areas. No significant differences regarding eccentricity index were observed between areas with and without evaginations. For detailed results see also Table 5.

Table 3
Procedural data of the index PCI.

Variable	All patients ($n = 16$)	Evagination group ($n = 8$)	Control group ($n = 8$)	p-Value
Scaffolds	20	10	10	>0.99
Non-compliant balloon pre-dilatation				
Performed	20 (100%)	10 (100%)	10 (100%)	>0.99
Balloon length (mm)	20 ± 6	19 ± 5	20 ± 6	0.83
Balloon diameter (mm)	2.9 ± 0.5	3 ± 0.4	2.8 ± 0.4	0.35
Inflation pressure (bar)	15 ± 4	15 ± 3	14 ± 4	0.74
Scaffold implantation				
Scaffold length (mm)	20 ± 7	21 ± 7	20 ± 6	0.65
Scaffold diameter (mm)	3.2 ± 0.4	3.2 ± 0.4	3.1 ± 0.4	0.92
Inflation pressure (bar)	12 ± 2	12 ± 2	11 ± 3	0.47
Non-compliant balloon post-dilatation				
Performed	20 (100%)	10 (100%)	10 (100%)	>0.99
Balloon length (mm)	14 ± 4	14 ± 3	14 ± 4	0.89
Balloon diameter (mm)	3.1 ± 1.2	3.2 ± 0.3	3.1 ± 1.3	0.54
Inflation pressure (bar)	16 ± 6	17 ± 4	16 ± 8	0.34

Values are mean ± standard deviation or n (%).

Table 4
Optical coherence tomography at follow-up: evagination vs. control group (all values normalized to nominal scaffold dimensions at implantation).

	Evagination group	Control group	p-Value
Mean scaffold area (mm^2)	15.8 ± 3.3	14.3 ± 3.4	0.09
Mean lumen area (mm^2)	16.3 ± 2.5	13.5 ± 3.1	0.03
Mean scaffold diameter (mm)	3.3 ± 0.5	3.1 ± 0.4	0.24
Normalized scaffold area	1.36 ± 0.60	1.13 ± 0.43	<0.001
Normalized lumen area	1.19 ± 0.58	0.77 ± 0.38	<0.001
Normalized scaffold diameter	1.17 ± 0.33	1.04 ± 0.19	<0.001
Mean eccentricity index	0.85 ± 0.05	0.85 ± 0.07	0.76
Sum of struts (n)	1242 ± 120	1326 ± 366	0.41
Strut fractures per frame	0.08 ± 0.11	0.02 ± 0.18	0.03
Malapposed struts per frame	0.13 ± 0.24	0.03 ± 0.07	0.006
Proximal edge dissection (n)	0	0	>0.99
Distal edge dissection (n)	0	0	>0.99

Values are mean ± standard deviation or n (%).

In BRS with evaginations, mean lumen area (Pearson correlation coefficient: 0.47; $p < 0.001$), scaffold area (Pearson correlation coefficient: 0.52; $p < 0.001$), and scaffold diameter (Pearson correlation coefficient: 0.74; $p < 0.001$) were significantly correlated with the time since scaffold implantation. Similar correlation could not be observed for the number of evaginations, evagination area or evagination depth. This strongly suggests that evaginations are progressive over time and that vessel and scaffold expansion (along the entire length of the scaffold) follow the process. In the control group, there was no significant correlation between lumen area, scaffold area or scaffold diameter and the time since scaffold implantation (see also Fig. 2). For detailed results see Table 6.

4. Discussion

BRS with evaginations are associated with significantly larger mean scaffold areas and scaffold diameters than BRS which do not develop evaginations. In addition, BRS with evaginations are associated with increased rates of strut fracture and malapposition as compared to those without.

One major finding of this study is that while peri-scaffold evaginations occur locally and not over the complete length of an affected scaffold, vessel and scaffold expansion occur not only in the segments affected by evaginations, but along the entire length of the implanted scaffold. Some extent of vessel remodeling after BRS implantation has been described in previous studies. However, this typically does not result in a significant lumen gain as compared to baseline lumen or scaffold dimensions [2,14]. As a second major finding, the enlargements of scaffold area, scaffold diameter, and lumen area in BRS with major

Table 5
Optical coherence tomography at follow-up: comparison of segments with and without evaginations within affected scaffolds.

	Scaffold segments with evaginations	Scaffold segments without evaginations	p-Value
Normalized scaffold area	1.37 ± 0.45	1.36 ± 0.64	0.41
Normalized lumen area	1.38 ± 0.49	1.13 ± 0.59	<0.001
Normalized scaffold diameter	1.18 ± 0.37	1.16 ± 0.20	0.33
Mean eccentricity index	0.86 ± 0.07	0.86 ± 0.08	0.58
Sum of struts (n)	202 ± 61	1023 ± 366	<0.001
Length (mm)	3.8 ± 1.6	16.7 ± 4.1	<0.001
Strut fractures per frame	0.23 ± 0.31	0.04 ± 0.19	0.02
Malapposed struts per frame	0.41 ± 0.36	0.13 ± 0.07	0.003
Proximal edge dissection (n)	0	0	>0.99
Distal edge dissection (n)	0	0	>0.99
Evagination area per cross-section (mm^2)	0.96 ± 1		
Evaginations per cross-section (n)	1.49 ± 0.76		
Evagination depth (mm)	0.48 ± 0.2		

Values are mean ± standard deviation or n (%).

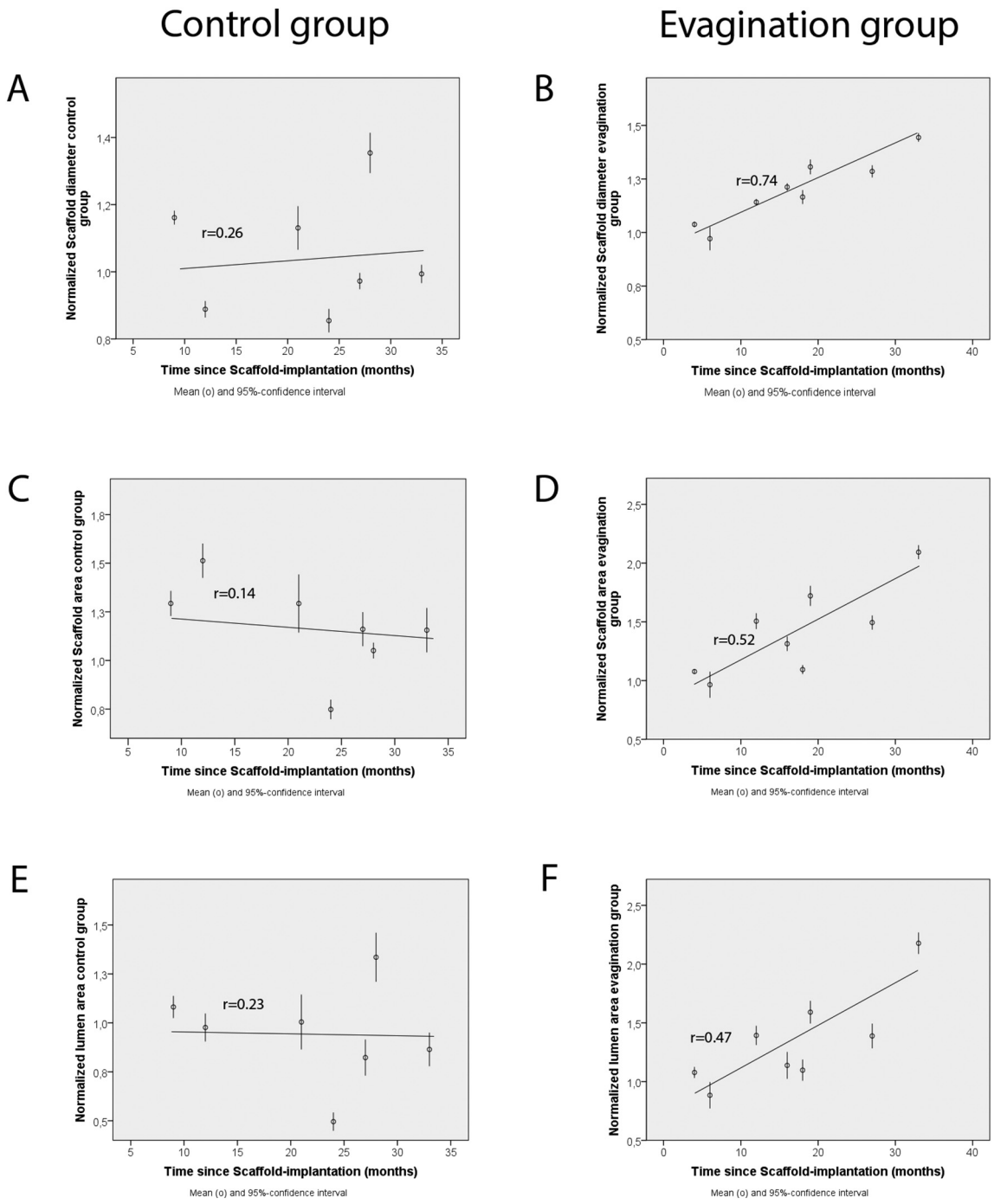

Fig. 2. Correlation of scaffold and vessel dimensions with the time since implantation. A and B. Normalized scaffold diameters relative to the time since scaffold implantation for the control (A) and evagination group (B). C and D. Normalized scaffold area relative to the time since scaffold implantation for the control (C) and evagination group (D). E and F. Normalized lumen area relative to the time since scaffold implantation for the control (D) and evagination group (E). Values are mean (o) and 95%-confidence interval. Line of best fit is shown for each graph; r = Pearson correlation coefficient.

Table 6
Correlation in the course of time since scaffold implantation.

	Evagination group		Control group	
	Pearson correlation coefficient	p-Value	Pearson correlation coefficient	p-Value
Lumen area	0.47	<0.001	0.23	0.54
Scaffold area	0.52	<0.001	0.14	0.32
Scaffold diameter	0.74	<0.001	0.26	0.63
Mean eccentricity index	0.08	0.22	0.13	0.72
Evaginations per cross-section (n)	0.03	0.60	0.23	0.43
Evagination area per cross-section (mm^2)	0.064	0.32	0.06	0.14
Evagination depth	0.025	0.701	0.32	0.87

evaginations significantly correlate with the time since scaffold implantation, which suggests that the process is continuous and progressive, with overexpansion of the vessel wall resulting in a consecutive enlargement of the scaffold. This does not occur to the same extent in scaffolds without evaginations. A recently published case report supports this hypothesis [15]. Well covered scaffold struts are incorporated into the vessel wall and degradation of the scaffolds´ poly-lactic structure over the course of time [16,17] may allow its struts to follow vessel enlargement (Fig. 3). On the other hand, evagination area, number of evaginations, and evagination depth show no significant correlation to the time since implantation. Based on our data, the process is likely initiated shortly after implantation and continues progressively thereafter.

Coronary evaginations are nearly absent in newer-generation DES, but frequently occurred in first-generation DES [4]. Gori et al. recently analyzed 102 BRS 12 months after implantation using OCT and reported that some extent of coronary evagination is present in about 54% of BRS [3]. However, Gori et al. performed OCT as part of a routine BRS follow-up protocol and used a definition of "evaginations" at a substantially lower threshold than we did. They defined evaginations as any "hollow" or outpouch in the vessel contour between well-apposed struts. Major evaginations, defined as having a depth >10% of the scaffold diameter and extending over a length >3 mm and BRS-aneurysms, defined as in-scaffold diameter >1.5-times of the reference vessel diameter, were only found in 5 of the 102 BRS analyzed by Gori et al. In contrast to this study, we included patients in whom evaginations had been detected angiographically at follow up. Patients with only minor outpouches and small evaginations were therefore not included in our cohort. The mean depth of evaginations in our study hence was 0.48 ± 0.2 mm extending over a length of 3.8 ± 1.6 mm. All of the BRS in our study fulfilled the criteria for the presence of major evaginations as defined by Gori et al. The association between strut fractures and malapposition with the occurrence of evaginations we found in our study (and which is more likely a consequence than a cause of the evaginations) was also described by Gori et al. Importantly, the correlation between scaffold area, scaffold diameter, and lumen area with the time since scaffold implantation is an entirely new finding of our study.

4.1. Limitations

We are aware that this study has some important limitations. It is a retrospective single-center analysis with a small number of patients and BRS. Patients were recruited into the analysis if evaginations were identified by angiography, which substantially favours large evaginations. OCT had not been performed in context with the baseline implantation. Therefore, reference vessel dimensions as determined by QCA at implantation were taken as baseline values for lumen and scaffold area. Baseline OCT would have been a better comparator. However, this systematic limitation affects both the group of patients with evaginations as well as the control cohort. Therefore, the main study findings are likely not influenced. Given the observational nature of our study, we cannot conclude whether the observed association of strut fractures (and malapposition) with evaginations is one of cause or effect. Since, in comparison to unaffected BRS, both were more frequent only in segments with evaginations, while vessel and scaffold expansion occurred over the entire length of the device, both strut fracture and malapposition are more likely a consequence of than a reason for evaginations. A potential limitation resides in the fact that with all follow-up angiograms and OCT procedures clinically driven, there is a bias towards

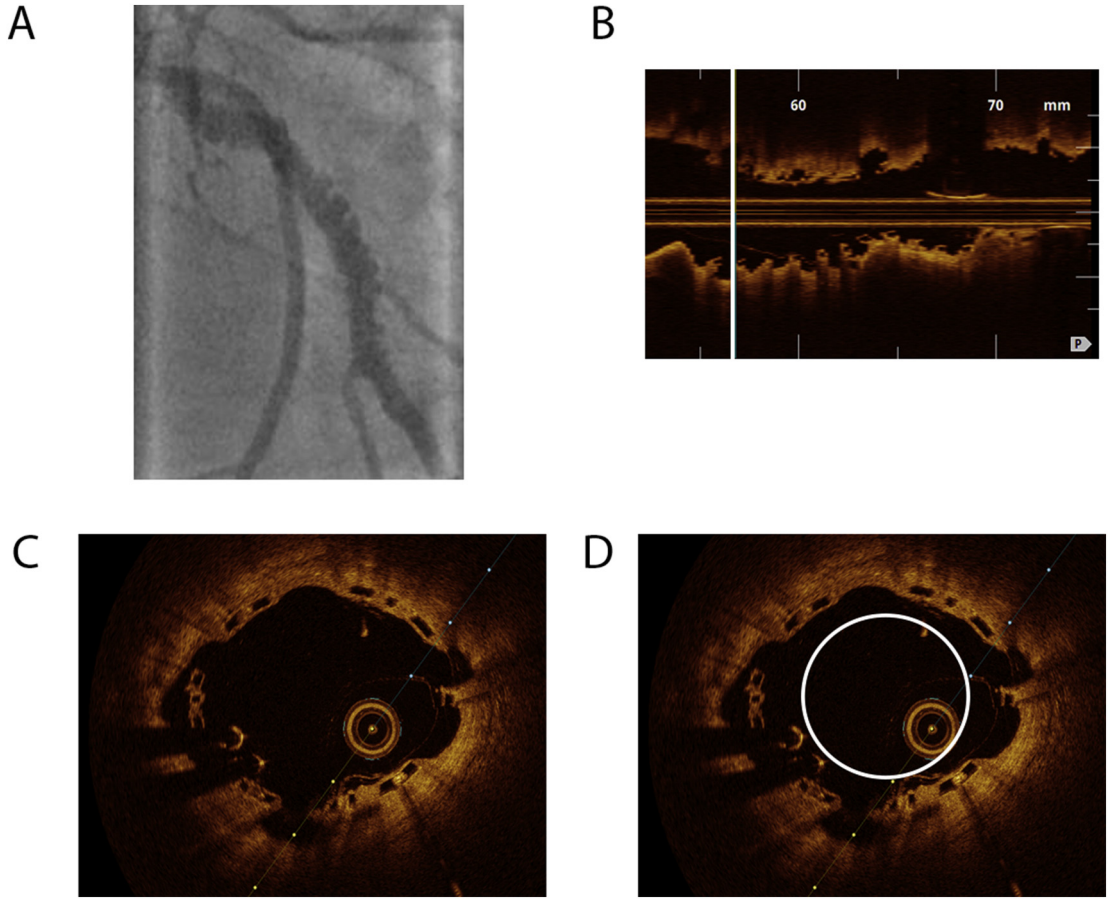

Fig. 3. Absorb BVS™ showing major coronary evaginations. A. Coronary angiogram of a 3.0/28 mm Absorb BVS™ 33 months after implantation into the circumflex artery. Evaginations are marked in white. B shows the longitudinal section of the affected BRS in the OCT. C shows an OCT cross-section (position: white mark in B) of the BRS with evaginations. In panel D the nominal scaffold size at implantation is indicated in white. Mean BRS-diameter (4.16 mm) is about 40% larger as compared to nominal size at implantation (3.0 mm).

the presence of in-scaffold restenosis in the control group. Our comparisons therefore are not comparisons to a "normal" control group. Finally, our analysis of time from baseline and extent of vessel enlargement rests on individual patients investigated at various intervals, and not the same patients imaged repetitively. However, effects are strong enough to at least be considered hypothesis-generating. Recently published reports of single cases support our findings [10–12,15].

4.2. Clinical implications

Coronary evaginations disturb laminar flow and may constitute a risk factor for late stent or scaffold thrombosis [8,9]. With some trials and analyses suggesting a slightly higher rate of scaffold thrombosis and target vessel major adverse cardiac events as compared to DES [18–23], coronary evaginations may be part of the underlying reason. Additionally, it is noteworthy that the observed overexpansion of the vessel may pose a particular challenge for future PCI of these segments, since in some cases diameters may grow too large to be treated with available devices.

Specific clinical and therapeutic implications of peri-scaffold evaginations and especially of the observed vessel overexpansion over the course of time will need further investigation.

5. Conclusion

Coronary evaginations as a consequence of PCI with bioresorbable vascular scaffolds are associated with progressive lumen enlargement that affects the entire scaffold length. Areas with evaginations are associated with higher rates of strut fracture and malapposed struts as compared to normal segments. The area of scaffolds affected by evaginations increases over time, suggesting that continuous degradation of the BRS allows its struts to follow the vascular expansion. "Coronary aneurysms" observed in patients late after BRS implantation may be a consequence of progressive vessel enlargement, followed by scaffold expansion, in the context of coronary evaginations.

Declaration of interests

None.

References

[1] Iqbal J, Onuma Y, Ormiston J, Abizaid A, Waksman R, Serruys P. Bioresorbable scaffolds: rationale, current status, challenges, and future. Eur Heart J 2014;35(12):765–76.
[2] Simsek C, Karanasos A, Magro M, et al. Long-term invasive follow-up of the everolimus-eluting bioresorbable vascular scaffold: five-year results of multiple invasive imaging modalities. EuroIntervention 2016;11(9):996–1003.
[3] Gori T, Jansen T, Weissner M, et al. Coronary evaginations and peri-scaffold aneurysms following implantation of bioresorbable scaffolds: incidence, outcome, and optical coherence tomography analysis of possible mechanisms. Eur Heart J 2016;37(26):2040–9.
[4] Radu MD, Räber L, Kalesan B, et al. Coronary evaginations are associated with positive vessel remodelling and are nearly absent following implantation of newer-generation drug-eluting stents: an optical coherence tomography and intravascular ultrasound study. Eur Heart J 2014;35(12):795–807.
[5] Joner M, Finn AV, Farb A, et al. Pathology of drug-eluting stents in humans: delayed healing and late thrombotic risk. J Am Coll Cardiol 2006;48(1):193–202.
[6] Cook S, Windecker S. Early stent thrombosis: past, present, and future. Circulation 2009;119(5):657–9.
[7] Guagliumi G, Sirbu V, Musumeci G, et al. Examination of the in vivo mechanisms of late drug-eluting stent thrombosis: findings from optical coherence tomography and intravascular ultrasound imaging. J Am Coll Cardiol Intv 2012;5(1):12–20.
[8] Räber L, Baumgartner S, Garcia-Garcia HM, et al. Long-term vascular healing in response to sirolimus- and paclitaxel-eluting stents: an optical coherence tomography study. J Am Coll Cardiol Intv 2012;5(9):946–57.
[9] Radu MD, Pfenniger A, Räber L, et al. Flow disturbances in stent-related coronary evaginations: a computational fluid-dynamic simulation study. EuroIntervention 2014;10(1):113–23.
[10] Cortese B, Silva Orrego P, Virmani R. Late coronary BVS malapposition and aneurysm: a time for appraisal. Catheter Cardiovasc Interv 2015;86(4):678–81.
[11] Timmers L, Lim YC, Tan HC, Low AF. Coronary aneurysm without malapposition after bioresorbable vascular scaffold implantation. EuroIntervention 2016;12(1):60.
[12] O'Gallagher K, Nerla R, Hill J, Byrne J. Acquired coronary artery aneurysm following treatment with bioresorbable vascular scaffolds. EuroIntervention 2016;12(9):1174.
[13] Gori T, Schulz E, Hink U, et al. Clinical, angiographic, functional, and imaging outcomes 12 months after implantation of drug-eluting bioresorbable vascular scaffolds in acute coronary syndromes. J Am Coll Cardiol Intv 2015;8(6):770–7.
[14] Diletti R, Farooq V, Girasis C, et al. Clinical and intravascular imaging outcomes at 1 and 2 years after implantation of absorb everolimus eluting bioresorbable vascular scaffolds in small vessels. Late lumen enlargement: does bioresorption matter with small vessel size? Insight from the ABSORB cohort B trial. Heart 2013;99(2):98–105.
[15] Nakatani S, Ishibashi Y, Suwannasom P, et al. Development and receding of a coronary artery aneurysm after implantation of a fully bioresorbable scaffold. Circulation 2015;131(8):764–7.
[16] Otsuka F, Pacheco E, Perkins LE, et al. Long-term safety of an everolimus-eluting bioresorbable vascular scaffold and the cobalt-chromium XIENCE V stent in a porcine coronary artery model. Circ Cardiovasc Interv 2014;7(3):330–42.
[17] Gomez-Lara J, Brugaletta S, Diletti R, et al. A comparative assessment by optical coherence tomography of the performance of the first and second generation of the everolimus-eluting bioresorbable vascular scaffolds. Eur Heart J 2011;32(3):294–304.
[18] Tröbs M, Achenbach S, Röther J, Klinghammer L, Schlundt C. Bioresorbable vascular scaffold thrombosis in a consecutive cohort of 550 patients. Catheter Cardiovasc Interv 2016. https://doi.org/10.1002/ccd.26569 [Epub ahead of print].
[19] Brugaletta S, Gori T, Low AF, et al. Absorb bioresorbable vascular scaffold versus everolimus-eluting metallic stent in ST-segment elevation myocardial infarction: 1-year results of a propensity score matching comparison: the BVS-EXAMINATION Study (bioresorbable vascular scaffold-a clinical evaluation of everolimus eluting coronary stents in the treatment of patients with ST-segment elevation myocardial infarction). J Am Coll Cardiol Intv 2015;8(1 Pt B):189–97.
[20] Gori T, Schulz E, Münzel T. Immediate, acute, and subacute thrombosis due to incomplete expansion of bioresorbable scaffolds. J Am Coll Cardiol Intv 2014;7(10):1194–5.
[21] Mukete BN, van der Heijden LC, Tandjung K, et al. Safety and efficacy of everolimus-eluting bioresorbable vascular scaffolds versus durable polymer everolimus-eluting metallic stents assessed at 1-year follow-up: a systematic review and meta-analysis of studies. Int J Cardiol 2016;221:1087–94.
[22] Lipinski MJ, Escarcega RO, Baker NC, et al. Scaffold thrombosis after percutaneous coronary intervention with ABSORB bioresorbable vascular scaffold: a systematic review and meta-analysis. J Am Coll Cardiol Intv 2016;9(1):12–24.
[23] Cassese S, Byrne RA, Ndrepepa G, et al. Everolimus-eluting bioresorbable vascular scaffolds versus everolimus-eluting metallic stents: a meta-analysis of randomised controlled trials. Lancet 2016;387(10018):537–44.